

Exact and approximate ensemble treatments of thermal pairing in a multilevel model

N. Quang Hung^{1*} and N. Dinh Dang^{1,2†}

1) Heavy-Ion Nuclear Physics Laboratory,

RIKEN Nishina Center for Accelerator-Based Science,

2-1 Hirosawa, Wako City, 351-0198 Saitama, Japan

2) Institute for Nuclear Science and Technique, Hanoi, Vietnam

(Dated: June 21, 2018)

Abstract

A systematic comparison is conducted for pairing properties of finite systems at nonzero temperature as predicted by the exact solutions of the pairing problem embedded in three principal statistical ensembles, as well as the unprojected (FTBCS1+SCQRPA) and Lipkin-Nogami projected (FTLN1+SCQRPA) theories that include the quasiparticle number fluctuation and coupling to pair vibrations within the self-consistent quasiparticle random-phase approximation. The numerical calculations are performed for the pairing gap, total energy, heat capacity, entropy, and microcanonical temperature within the doubly-folded equidistant multilevel pairing model. The FTLN1+SCQRPA predictions agree best with the exact grand-canonical results. In general, all approaches clearly show that the superfluid-normal phase transition is smoothed out in finite systems. A novel formula is suggested for extracting the empirical pairing gap in reasonable agreement with the exact canonical results.

PACS numbers: 21.60.-n, 21.60.Jz, 24.60.-k, 24.10.Pa, 21.10.Ma

*On leave of absence from the Institute of Physics and Electronics, Hanoi, Vietnam; Electronic address:

nqhung@riken.jp

†Electronic address: dang@riken.jp

I. INTRODUCTION

Pairing correlations are a fundamental feature responsible for the superconducting (superfluid) properties in many-body systems ranging from very large ones as neutron stars to tiny ones as atomic nuclei. In macroscopic systems such as superconductors, pairing correlations are destroyed as the temperature T increases and completely vanish at a value $T_c \simeq 0.57\Delta(0)$, which is the critical temperature of the phase transition from the superfluid state to the normal one. Here $\Delta(0)$ is the value of the pairing gap at $T = 0$. The recent years witness a renewed interest in pairing correlations, which is supported by the exact solutions of the pairing problem in practice, the studies of unstable nuclei, the BCS to Bose-Einstein condensation crossover, etc.

The superfluid properties and superfluid-normal (SN) phase transition of infinite systems are accurately described by the Bardeen-Cooper-Schrieffer theory [1], where the average within the grand canonical ensemble (GCE) is used to obtain the occupation number in the form of Fermi-Dirac distribution for noninteracting fermions. The GCE consists of identically prepared systems in thermal equilibrium, each of which shares its energy and number of particles with an external heat bath. As compared to the other two principal thermodynamic ensembles, namely the canonical ensemble (CE) and the microcanonical one (MCE), the GCE is, perhaps, the most popular in theoretical studies of systems at finite temperature because it is very convenient in the calculations of average thermodynamic quantities¹. The CE is also in contact with the heat bath, but the particle number is the same for all systems. The MCE is an ensemble of thermally isolated systems sharing the same energy and particle number. In thermodynamics limit (i.e. when the system's particle number N and volume V approach infinity, but N/V is finite), fluctuations of energy and particle number are zero, therefore three types of ensembles offer the same average values for thermodynamic quantities. Thermodynamics limit works quite well in large systems as well where these fluctuations are negligible. The discrepancies between the predictions by three types of ensembles arise when thermodynamics is applied to small systems such as atomic nuclei or nanometer-size clusters. These systems have a fixed and not very large number of

¹ For instance, the double-time Green's functions $G(t, t')$, which are defined by using the GCE [2], depend only on the time difference $(t - t')$, which greatly simplify the derivations in many statistical physics applications.

particles, their single-particle energy spectra are discrete with the level spacing comparable to the pairing gap. Under this circumstance, the justification of using the GCE for these systems becomes questionable. A number of theoretical studies have also shown that, in these tiny systems, thermal fluctuations become so large that they smooth out the sharp SN transition [3, 4, 5, 6, 7, 8, 9, 10]. As the result, the pairing gap never collapses but decreases monotonously with increasing T . These predictions are in qualitative agreement with the results obtained by averaging the pairing energy in the CE built on the eigenvalues obtained by exactly solving the pairing problem [11, 12]. As a matter of fact, even at $T = 0$, the exact pairing solution in nuclei shows a sizable pairing energy in the region where the BCS solution collapses [12]. In the literature so far, under the pretext that a nucleus is a system with a fixed number of particle, the thermodynamic averages of the exact solutions of the pairing Hamiltonian are usually carried out within the CE, and the results are compared with those obtained within different theoretical approximations at $T \neq 0$. The latter, such as the BCS, Hartree-Fock-Bogoliubov (HFB) theories, etc., as a rule, are always derived within the GCE, where both energy and particle number fluctuate. On the other hand, the well-known argument that the nuclear temperature should be extracted from the MCE of thermally isolated nuclei is also quite often debated and studied in detail [7].

These results suggest that a thorough comparison of the predictions offered by the exact pairing solutions averaged within three principal thermodynamic ensembles, and those given by the recent microscopic approaches, which include fluctuations around the thermal pairing mean field in nuclei, might be timely and useful. This question is not new, but the answers to it have been so far only partial. Already in the sixties Kubo [13] drew attention to the thermodynamic effects in very small metal particles. Later, Denton et al. [14] used Kubo's assumption to study the difference between the predictions offered by the GCE and CE for the heat capacity and spin susceptibility within a spinless equidistant level model for electrons. Very recently, the predictions for thermodynamic quantities such as total energy, heat capacity, entropy, and microcanonical temperature within three principal ensembles were studied and compared in Ref. [15] by using the exact solutions of an equidistant multilevel model with constant pairing interaction parameter. However, no results for the pairing gaps as functions of temperature are reported.

In the present paper, we carry out a systematic comparison of predictions for nuclear pairing properties obtained by averaging the exact solutions in three principal thermodynamic

ensembles as well as those offered by recent microscopic approaches to thermal pairing. For the latter, we choose the unprojected and particle-number projected versions of the FTBCS1+SCQRPA, which we recently developed in Ref. [9]. This approach has been rigorously derived based on the same variational procedure used for the derivation of the standard BCS theory, taking into account the effects due to quasiparticle-number fluctuation (QNF) and coupling to the self-consistent quasiparticle random-phase approximation (SCQRPA) in addition to those of the QNF.

The paper is organized as follows. The pairing Hamiltonian, its diagonalization, ensemble treatments of the exact pairing solutions, the main results of the FTBCS1 and FTBCS1+SCQRPA theories, as well as their particle-number projected versions, are summarized in Sec. II. The numerical results obtained within the doubly-folded equidistant multilevel model [11] are analyzed in Sec. III. The paper is summarized in the last section, where conclusions are drawn.

II. EXACT SOLUTION OF PAIRING HAMILTONIAN

A. Exact solution at zero temperature

We consider a system of N particles with single-particle energies ϵ_j , which are generated by particle creation operators a_{jm}^\dagger on j th orbitals with shell degeneracies $2\Omega_j$ ($\Omega_j = j + 1/2$), and interacting via a monopole-pairing force with a constant parameter G . This system is described by the well-known pairing Hamiltonian

$$H = \sum_{jm} \epsilon_j \hat{N}_j - G \sum_{jj'} \hat{P}_j^\dagger \hat{P}_{j'} , \quad (1)$$

where the particle-number operator \hat{N}_j and pairing operator \hat{P}_j are given as

$$\hat{N}_j = \sum_m a_{jm}^\dagger a_{jm} , \quad \hat{P}_j^\dagger = \sum_{m>0} a_{jm}^\dagger a_{j\tilde{m}}^\dagger , \quad \hat{P}_j = (\hat{P}_j^\dagger)^\dagger , \quad (2)$$

with the symbol $\tilde{}$ denoting the time-reversal operator, namely $a_{j\tilde{m}} = (-)^{j-m} a_{j-m}$. For a two-component system with Z protons and N neutrons, the sums in Eq. (1) run also over all $j_\tau m_\tau$, $j'_\tau m'_\tau$, and G_τ with $\tau = (Z, N)$.

The pairing Hamiltonian (1) was solved exactly for the first time in the sixties by Richardson [11]. By noticing that the operators $\hat{J}_j^z \equiv (\hat{N}_j - \Omega_j)/2$, $\hat{J}_j^+ \equiv \hat{P}_j^\dagger$, and $\hat{J}_j^- \equiv \hat{P}_j$ close

an SU(2) algebra of angular momentum, the authors of Ref. [12] have reduced the problem of solving the Hamiltonian (1) to its exact diagonalization in the subsets of representations, each of which is given by a set basis states $|k\rangle \equiv |\{s_j\}, \{N_j\}\rangle$ characterized by the partial occupation number $N_j \equiv (J_j^z + \Omega_j)/2$ and partial seniority (the number of unpaired particles) $s_j \equiv \Omega_j - 2N_j$ of the j th single-particle orbital. Here $J_j(J_j + 1)$ is the eigenvalue of the total angular momentum operator $(\hat{J}_j)^2 \equiv \hat{J}_j^+ \hat{J}_j^- + \hat{J}_j^z(\hat{J}_j^z - 1)$. The partial occupation number N_j and seniority s_j are bound by the constraints of angular momentum algebra $s_j \leq N_j \leq 2\Omega_j - s_j$ with $s_j \leq \Omega_j$. In the present paper, we use this exact diagonalization method to find the eigenvalues \mathcal{E}_s and eigenstates (eigenvectors) $|s\rangle$ of Hamiltonian (1). Each s th eigenstate $|s\rangle$ is fragmented over the basis states $|k\rangle$ according to $|s\rangle = \sum_k C_k^{(s)} |k\rangle$ with the total seniority $s = \sum_j s_j$, and degenerated by

$$d_s = \prod_j \left[\frac{(2\Omega_j)!}{s_j!(2\Omega_j - s_j)!} - \frac{(2\Omega_j)!}{(s_j - 2)!(2\Omega_j - s_j + 2)!} \right], \quad (3)$$

where $(C_k^{(s)})^2$ determine the weights of the eigenvector components. The state-dependent exact occupation number $f_j^{(s)}$ on the j th single-particle orbital is then calculated as the average value of partial occupation numbers $N_j^{(k)}$ weighted over the basis states $|k\rangle$ as

$$f_j^{(s)} = \frac{\sum_k N_j^{(k)} (C_k^{(s)})^2}{\sum_k (C_k^{(s)})^2} = \sum_k N_j^{(k)} (C_k^{(s)})^2, \quad \text{with} \quad \sum_k (C_k^{(s)})^2 = 1. \quad (4)$$

B. Exact solution embedded in thermodynamic ensembles

The properties of the nucleus as a system of N interacting fermions at energy \mathcal{E} can be extracted from its level density $\rho(\mathcal{E}, N)$ [16]

$$\rho(\mathcal{E}, N) = \sum_{s,n} \delta(\mathcal{E} - \mathcal{E}_s^{(n)}) \delta(N - n), \quad (5)$$

where $\mathcal{E}_s^{(n)}$ are the energies of the quantum states $|s\rangle$ of the n -particle system. Applying to the pairing problem, these energies are the eigenvalues, which are obtained by exactly diagonalizing the pairing Hamiltonian (1), as has been discussed in the previous section.

1. Grand canonical and canonical ensembles

Since each system in a GCE is exchanging its energy and particle number with the heat bath at a given temperature $T = 1/\beta$, both of its energy and particle number are allowed

to fluctuate. Therefore, instead of the level density (5), it is convenient to use the average value, which is obtained by integrating (5) over the intervals in \mathcal{E} and N . This Laplace transform of the level density $\rho(\mathcal{E}, N)$ defines the grand partition function $Z(\beta, \lambda)$ [16],

$$\mathcal{Z}(\beta, \lambda) = \iint_0^\infty \rho(\mathcal{E}, N) e^{-\beta(\mathcal{E} - \lambda N)} dN d\mathcal{E} = \sum_n e^{\beta \lambda n} Z(\beta, n), \quad (6)$$

where $Z(\beta, n)$ denotes the partition function of the CE at temperature T and particle number fixed at n , namely

$$Z(\beta, n) = \sum_s p_s(\beta, n), \quad p_s(\beta, n) = d_s^{(n)} e^{-\beta \mathcal{E}_s^{(n)}}. \quad (7)$$

Within the GCE, the chemical potential λ should be chosen as a function of T so that the average particle number $\langle N \rangle$ of the system always remains equal to N . The summations over n and s in Eqs. (6) and (7) are obtained by using Eq. (5) taking into account the degeneracy $d_s^{(n)}$ (3) of each s th state in the n -particle system, and carrying out the double integration with δ functions.

The thermodynamic quantities such as total energy \mathcal{E} , heat capacity C within the GCE and CE are as usual given as

$$\langle \mathcal{E} \rangle_\alpha = -\frac{\partial \ln \mathbf{Z}(\beta)_\alpha}{\partial \beta}; \quad C^{(\alpha)} = \frac{\partial \langle \mathcal{E} \rangle_\alpha}{\partial T} \quad (8)$$

where $\alpha = \text{GC}$ for the GCE and $\alpha = \text{C}$ for the CE.

The thermodynamic entropy $S_{\text{th}}^{(\alpha)}$ is calculated within the GCE or CE based on the general definition of the change of entropy (by Clausius):

$$dS = \beta d\mathcal{E}. \quad (9)$$

By using the differentials of $\ln \mathbf{Z}(\beta)_\alpha$, one obtains

$$S_{\text{th}}^{(\text{GC})} = \beta(\langle \mathcal{E} \rangle_{\text{GC}} - \lambda N) + \ln \mathcal{Z}(\beta, \lambda), \quad S_{\text{th}}^{(\text{C})} = \beta \langle \mathcal{E} \rangle_{\text{C}} + \ln Z(\beta, N). \quad (10)$$

The occupation number f_j on the j th single-particle orbital is obtained as the ensemble average of the state-dependent occupation numbers $f_j^{(s)}$, namely

$$f_j^{(\text{GC})} = \frac{1}{\mathcal{Z}(\beta, \lambda)} \sum_{s,n} f_j^{(s,n)} d_s^n e^{-\beta(\mathcal{E}_s^{(n)} - \lambda n)}, \quad f_j^{(\text{C})} = \frac{1}{Z(\beta, N)} \sum_s f_j^{(s,N)} d_s^N e^{-\beta \mathcal{E}_s^N}, \quad (11)$$

for the GCE and CE, respectively.

2. Microcanonical ensemble

Different from the GCE and CE, there is no heat bath within the MCE. A MCE consists of thermodynamically isolated systems, each of which may be in a different microstate (microscopic quantum state) $|s\rangle$, but has the same total energy \mathcal{E} and particle number N . Since the energy and particle number of the system are fixed, one should use the level density (5) to calculate directly the entropy by Boltzmann's definition, namely

$$S^{(\text{MC})}(\mathcal{E}) = \ln \Omega(\mathcal{E}) , \quad (12)$$

where $\Omega(\mathcal{E}) = \rho(\mathcal{E})\Delta\mathcal{E}$ is the statistical weight, i.e. the number of eigenstates of Hamiltonian (1) within a fixed energy interval $\Delta\mathcal{E}$. The condition of thermal equilibrium then leads to the standard definition of temperature within the MCE as [16]

$$\beta = \frac{\partial S^{(\text{MC})}(\mathcal{E})}{\partial \mathcal{E}} = \frac{1}{\rho(\mathcal{E})} \frac{\partial \rho(\mathcal{E})}{\partial \mathcal{E}} , \quad (13)$$

using which one can build a “thermometer” for each value of the excitation energy \mathcal{E} of the system.

In practical calculations, to handle the numerical derivative at the right-hand side of Eq. (13), one needs a continuous energy dependence of $\rho(\mathcal{E})$ in the form of a distribution in Eq. (5). This is realized by replacing the Dirac- δ function $\delta(x)$ at the right-hand side of Eq. (5), where $x \equiv \mathcal{E} - \mathcal{E}_s$, with a nascent δ -function $\delta_\sigma(x)$ ($\sigma > 0$), i.e. a function that becomes the original $\delta(x)$ in the limit $\sigma \rightarrow 0$ ². Among the popular nascent δ functions are the Gaussian (or normal) distribution, Breit-Wigner distribution [21], and Lorentz (or relativistic Breit-Wigner) distribution, which are given as

$$\begin{aligned} \delta_\sigma(x)_G &= \frac{1}{\sigma\sqrt{2\pi}} e^{-\frac{x^2}{2\sigma^2}} , \quad \delta_\sigma(x)_{\text{BW}} = \frac{1}{\pi} \frac{\sigma}{x^2 + \sigma^2} , \\ \delta_\sigma(\mathcal{E} - \mathcal{E}_s)_L &= \frac{1}{\pi} \frac{\sigma\mathcal{E}^2}{(\mathcal{E}^2 - \mathcal{E}_s^2)^2 + \sigma^2\mathcal{E}^2} , \end{aligned} \quad (14)$$

respectively. In these distributions, σ is a parameter, which defines the width of the peak centered at $\mathcal{E} = \mathcal{E}_s$. The full widths at the half maximum (FWHM) Γ of these distributions are $\Gamma = 2\sigma\sqrt{2\ln 2} \simeq 2.36\sigma$ for the Gaussian distribution, and 2σ for the Breit-Wigner and

² This replacement is equivalent to the folding procedure for the average density, discussed in Sec. 2.9.3 of the textbook [17], taken at zero degree ($M = 0$) of the Laguerre polynomial $L_M^{1/2}(x)$.

Lorentz ones. The disadvantage of using such smoothing is that the temperature extracted from Eq. (13), of course, depends on the chosen distribution as well as the value of the parameter σ . It is worth mentioning that changing σ is not equivalent to changing ΔE for the discrete $\rho(\mathcal{E})$ used in calculating the statistical weight $\Omega(\mathcal{E})$ in Eq. (12), since the wings of any distributions in Eq. (14) extend with increasing σ , whereas for the discrete spectrum, no more levels might be found in the low \mathcal{E} by enlarging $\Delta\mathcal{E}$.

The generalized form of Boltzmann's entropy (12) is the definition by von Neumann

$$S = -\text{Tr}[\rho \ln \rho] , \quad (15)$$

which is the quantum mechanical correspondent of the Shannon's entropy in classical theory. By expressing the level density $\rho(\mathcal{E})$ in Eq. (5) in terms of the local densities of states $F_k(\mathcal{E})$ [7],

$$\rho(\mathcal{E}) = \sum_k F_k(\mathcal{E}) , \quad F_k(\mathcal{E}) = \sum_s [C_k^{(s)}]^2 \delta(\mathcal{E} - \mathcal{E}_s) , \quad (16)$$

the entropy becomes

$$S^{(s)} = - \sum_k [C_k^{(s)}]^2 \ln [C_k^{(s)}]^2 . \quad (17)$$

By using Eqs. (13) and (17) one can extract a quantity T_s as the “microcanonical temperature of each eigenstate s ”.

C. Determination of pairing gaps from total energies

1. Ensemble-averaged pairing gaps

Although the exact solution of Hamiltonian (1) does not produce a pairing gap *per se*, which is a quantity determined within the mean field, it is useful to define an ensemble-averaged pairing gap to be closely compared with the gaps predicted by the approximations within and beyond the mean field. In the present paper, we define this ensemble-averaged gap Δ_α from the pairing energy $\mathcal{E}_{\text{pair}}^{(\alpha)}$ of the system as follows

$$\Delta_\alpha = \sqrt{-G\mathcal{E}_{\text{pair}}^{(\alpha)}} , \quad \mathcal{E}_{\text{pair}}^{(\alpha)} = \langle \mathcal{E} \rangle_\alpha - \langle \mathcal{E} \rangle_\alpha^{(0)} , \quad \langle \mathcal{E} \rangle_\alpha^{(0)} \equiv 2 \sum_j \Omega_j \left[\epsilon_j - \frac{G}{2} f_j^{(\alpha)} \right] f_j^{(\alpha)} , \quad (18)$$

within the GCE ($\alpha = \text{GC}$), CE ($\alpha = \text{C}$), and MCE ($\alpha = \text{MC}$), where for the latter we put $\mathcal{E}_{\text{pair}}^{(\alpha)} \equiv \mathcal{E}_{\text{pair}}(s)$ with $\langle \mathcal{E} \rangle_{\text{MC}} \equiv \mathcal{E}_s^{(N)}$. The term $\langle \mathcal{E} \rangle_\alpha^{(0)}$ denotes the contribution from the

energy $2 \sum_j \Omega_j \epsilon_j f_j^{(\alpha)}$ of the single-particle motion described by the first term at the right-hand side of Hamiltonian (1), and the energy $-G \sum_j \Omega_j [f_j^{(\alpha)}]^2$ of uncorrelated single-particle configurations caused by the pairing interaction in Hamiltonian (1). Therefore, subtracting the term $\langle \mathcal{E} \rangle_\alpha^{(0)}$ from the total energy $\langle \mathcal{E} \rangle_\alpha$ yields the residual that corresponds to the energy due to pure pairing correlations. By replacing $f_j^{(\alpha)}$ with v_j^2 , one recovers from Eq. (18) the expression $\mathcal{E}_{\text{pair}}^{(\text{BCS})} = -\Delta_{\text{BCS}}^2/G$ of the BCS theory. Given several definitions of the ensemble-averaged gap existing in the literature, it is worth mentioning that the definition (18) is very similar to that given by Eq. (52) of Ref. [18], whereas, even within the CE, the gap Δ_C is different from the canonical gap defined in Refs. [19, 20], since in the latter, the term $\langle \mathcal{E} \rangle_C^{(0)}$ is taken at $G = 0$. The pairing energy $\mathcal{E}_{\text{pair}}^{(\alpha)}$ in Eq. (18) is also different from the simple average value $-G \sum_{jj'} \langle \hat{P}_j^\dagger \hat{P}_{j'} \rangle_\alpha$ of the last term of Hamiltonian (1) as the latter still contains the uncorrelated term $-G \sum_j \Omega_j [f_j^{(\alpha)}]^2$.

2. Empirical determination of pairing gap at finite temperature

The simplest way to empirically determine the pairing gap of a system with N particles in the ground state (at $T = 0$) is to use the so-called three-point formula $\Delta^{(3)}(N)$, which is given by the odd-even mass difference between the ground-state energies of the N -particle system and the neighboring systems with $N \pm 1$ particles [16]. A straightforward extension of this formula to $T \neq 0$ reads

$$\Delta^{(3)}(\beta, N) \simeq \frac{(-1)^N}{2} [\langle \mathcal{E}(N+1) \rangle_\alpha - 2\langle \mathcal{E}(N) \rangle_\alpha + \langle \mathcal{E}(N-1) \rangle_\alpha] , \quad (19)$$

which was used, e.g., in Ref. [22] to extract the thermal pairing gaps in wolfram and molybdenum isotopes. The four-point formula represents the arithmetic average of the three-point gaps over in the neighboring systems with N and $N - 1$ particles, namely

$$\Delta^{(4)}(\beta, N) = \frac{1}{2} [\Delta^{(3)}(N) + \Delta^{(3)}(N-1)] . \quad (20)$$

A drawback of the gaps $\Delta^{(3)}(\beta, N)$ and $\Delta^{(4)}(\beta, N)$, defined in this way, is that they still contain the admixture with the contribution from uncorrelated single-particle configurations. The later increases with increasing T . Therefore, Eq. (19) and, consequently, Eq. (20) do not hold at finite temperature. To remove this contribution so that the experimentally extracted pairing gap is comparable with Δ_α in Eq. (18), we propose in the present paper

an improved odd-even mass difference formula at $T \neq 0$ as follows. Using Eq. (18) to express the total energy $\langle \mathcal{E}(N) \rangle_\alpha$ of the system in terms of $\Delta_\alpha(N)$ and $\langle \mathcal{E}(N) \rangle_\alpha^0$, we obtain

$$\langle \mathcal{E}(N) \rangle_\alpha = \langle \mathcal{E}(N) \rangle_\alpha^{(0)} - \frac{\tilde{\Delta}^2(\beta, N)}{G}. \quad (21)$$

where $\langle \mathcal{E}(N) \rangle_\alpha$ is the experimentally known total energy of the system with N particles at $T \neq 0$, whereas $\tilde{\Delta}(\beta, N)$ is the pairing gap of this system to be determined. Replacing $\langle \mathcal{E}(N) \rangle_\alpha$ in the definition of the odd-even mass difference (19) with the right-hand side of Eq. (21), we obtain a quadratic equation for the three-point $\tilde{\Delta}^{(3)}(\beta, N)$

$$\tilde{\Delta}^{(3)}(\beta, N) = (-1)^N \left\{ \frac{1}{2} [\langle \mathcal{E}(N+1) \rangle_\alpha + \langle \mathcal{E}(N-1) \rangle_\alpha] - \langle \mathcal{E} \rangle_\alpha^0 + \frac{[\tilde{\Delta}^{(3)}(\beta, N)]^2}{G} \right\}. \quad (22)$$

The discriminant of this equation is equal to $G\sqrt{1 - 4S'/G}$, where

$$S' = \frac{1}{2} [\langle \mathcal{E}(N+1) \rangle_\alpha + \langle \mathcal{E}(N-1) \rangle_\alpha] - \langle \mathcal{E}(N) \rangle_\alpha^{(0)}. \quad (23)$$

Therefore the condition for Eq. (22) to have real solutions is $S' \leq G/4$. Including both cases with even and odd N , the positive solution of Eq. (22) is always possible provided $S' < 0$, which reads

$$\tilde{\Delta}^{(3)}(\beta, N) = \frac{G}{2} \left[(-1)^N + \sqrt{1 - 4\frac{S'}{G}} \right]. \quad (24)$$

The quantity S' differs from the conventional odd-even mass difference shown in the square brackets of (19) by the contribution due to the uncorrelated single-particle motion, i.e. the last sum containing G in the definition of $\langle \mathcal{E} \rangle_\alpha^{(0)}$ in Eq. (18). The latter is zero only at $G = 0$, which yields $\tilde{\Delta}^{(3)}(\beta, N) = 0$, as can be seen from Eq. (24) as well. In this case both S' and the expression in the square brackets of Eq. (19) vanish as they are just the difference of the Hartree-Fock energies $\langle E(N+1) \rangle_\alpha^{(0)} + \langle E(N-1) \rangle_\alpha^{(0)} - 2\langle E(N) \rangle_\alpha^{(0)}$, which is zero at $G = 0$. Moreover, while the odd-even mass difference of Eq. (19) can be positive or negative depending on whether N is even or odd, S' should be always negative as discussed above. The gap $\tilde{\Delta}^{(3)}(\beta, N)$ extracted from Eq. (24) is, therefore, consistent with the result of the exact calculation at zero temperature, where the pairing gap is zero only at $G = 0$, and increases with G (See e.g. Fig. 1 - (a) of Ref. [15]). As compared to the simple finite-temperature extension of the odd-even mass (19), the modified gap $\tilde{\Delta}^{(3)}(\beta, N)$ is closer to the ensemble-averaged gap $\Delta_\alpha(N)$ (18) since it is free from the contribution of uncorrelated single-particle configurations. In Eq. (24), the energies $\langle \mathcal{E}(N+1) \rangle_\alpha$ and $\langle \mathcal{E}(N-1) \rangle_\alpha$ can be

extracted from experiments, whereas the pairing interaction parameter G can be obtained by fitting the experimental values of $\Delta(T = 0, N)$. The energy $\langle \mathcal{E}(N) \rangle_\alpha^{(0)}$ remains the only model-dependent quantity being determined in terms of the single-particle energies ϵ_j and single-particle occupation numbers $f_j^{(\alpha)}$. As a matter of fact, since the pairing gap $\Delta^{(3)}(\beta, N)$ of the N -particle system at the left-hand side of the expression (19) is also present in the total energy $\langle \mathcal{E}(N) \rangle_\alpha$ of the same system at the right-hand side of (19), the former is simply extracted from the latter by using Eqs. (18) and (21). As the result, the modified gap $\tilde{\Delta}^{(3)}(\beta, N)$ of the system with N particles explicitly depends now on $\langle \mathcal{E}(N) \rangle_\alpha^{(0)}$ of the same system rather than on its total energy $\langle \mathcal{E}(N) \rangle$. The modified four-point gap $\tilde{\Delta}^{(4)}(\beta, N)$ is then obtained from the modified three-point gaps $\tilde{\Delta}^{(3)}(\beta, N)$ and $\tilde{\Delta}^{(3)}(\beta, N - 1)$ by using the definition (20).

III. FTBCS1+SCQRPA AND FTLN1+SCQRPA

The FTBCS1+SCQRPA includes the effects due to quasiparticle-number fluctuation and coupling to the SCQRPA vibrations, which are neglected within the standard BCS theory. The derivation of the FTBCS1+SCQRPA has already been given and discussed in detail in Ref [9]. Therefore we give below only the main results, which are necessary to follow the numerical calculations in the present paper.

The rigorous derivation of the FTBCS1+SCQRPA theory follows the standard variational procedure, which is used to derived the BCS theory. By using the Bogoliubov's canonical transformation [23]

$$\alpha_{jm}^\dagger = u_j a_{jm}^\dagger - v_j a_{j\tilde{m}} , \quad \alpha_{j\tilde{m}} = u_j a_{j\tilde{m}} + v_j a_{jm}^\dagger , \quad (25)$$

the pairing Hamiltonian (1) is expressed in terms of quasiparticle operators, α_{jm}^\dagger and α_{jm} , as $H_{\text{q.p.}}$, whose explicit form is given in many papers, e.g., Eqs. (3), (8) – (14) of Ref. [9]. The u_j and v_j coefficients of the Bogoliubov's transformation (25) are determined by minimizing the GCE average value of the Hamiltonian $\mathcal{H} = H_{\text{q.p.}} - \lambda \hat{N}$. This leads to the equation

$$\langle [\mathcal{H}, \mathcal{A}_j^\dagger] \rangle_{\text{GC}} = 0 , \quad \text{where } \mathcal{A}_j^\dagger = \frac{1}{\sqrt{\Omega_j}} \sum_{j=1}^{\Omega_j} \alpha_{jm}^\dagger \alpha_{j\tilde{m}}^\dagger . \quad (26)$$

The final result yields the equation for the level-dependent pairing gap Δ_j for a system with

even number N of particles,

$$\Delta_j = \Delta + \delta\Delta_j, \quad \Delta = G \sum_{j'} \Omega_{j'} (1 - 2n_{j'}) u_{j'} v_{j'}, \quad \delta\Delta_j = 2G \frac{\delta\mathcal{N}_j^2}{1 - 2n_j} u_j v_j, \quad (27)$$

with the QNF defined as

$$\delta\mathcal{N}_j^2 \equiv n_j (1 - n_j), \quad (28)$$

and the equation for the average particle number N ,

$$N = 2 \sum_j \Omega_j [v_j^2 (1 - 2n_j) + n_j], \quad (29)$$

The u_j and v_j coefficients in Eqs. (27) and (29) are determined as

$$u_j^2 = \frac{1}{2} \left[1 + \frac{\epsilon'_j - Gv_j^2 - \lambda}{E_j} \right], \quad v_j^2 = \frac{1}{2} \left[1 - \frac{\epsilon'_j - Gv_j^2 - \lambda}{E_j} \right], \quad (30)$$

with the renormalized single-particle energies ϵ'_j ,

$$\epsilon'_j = \epsilon_j + \frac{G}{\sqrt{\Omega_j(1 - 2n_j)}} \sum_{j'} \sqrt{\Omega_{j'}} (u_{j'}^2 - v_{j'}^2) (\langle \mathcal{A}_j^\dagger \mathcal{A}_{j' \neq j}^\dagger \rangle + \langle \mathcal{A}_j^\dagger \mathcal{A}_{j'} \rangle), \quad (31)$$

and the quasiparticle energies

$$E_j = \sqrt{(\epsilon'_j - Gv_j^2 - \lambda)^2 + \Delta_j^2}. \quad (32)$$

For a system with an odd number of particles, the blocking effect caused by the unpaired particle should be taken into account in Eqs. (27) and (29). In the present paper, for simplicity, we do not consider systems with odd particle numbers within the FTBCS1+SCQRPA and FTLN1+SCQRPA.

The pair correlators $\langle \mathcal{A}_j^\dagger \mathcal{A}_{j' \neq j}^\dagger \rangle$ and $\langle \mathcal{A}_j^\dagger \mathcal{A}_{j'} \rangle$ in Eq. (31) are determined by numerically solving a set of coupled equations (47) and (48) of Ref. [9], which contain the \mathcal{X}_j^μ and \mathcal{Y}_j^μ amplitudes of the SCQRPA equations. The details of the derivation of the SCQRPA are given in Ref. [24]. The SCQRPA equations are solved self-consistently with the gap and number equations (27) and (29). The quasiparticle occupation numbers n_j are then found by solving a set of equations that include coupling of quasiparticle density operators $\alpha_{jm}^\dagger \alpha_{jm}$ to the SCQRPA phonon operators. The result yields the integral equation (69) of Ref. [9] for n_j . To compare with the level-independent gap such as the BCS one, the level-weighted gap,

$$\bar{\Delta} = \sum_j \Omega_j \Delta_j / \sum_j \Omega_j, \quad (33)$$

is used instead of Eq. (27). The total energy $\langle \mathcal{E} \rangle_{\text{FTBCS1+SCQRPA}}$ is calculated by averaging the quasiparticle representation $H_{\text{q.p.}}$ of the Hamiltonian (1) within the GCE, i.e.

$$\langle \mathcal{E} \rangle = \langle H_{\text{q.p.}} \rangle_{\text{GC}} , \quad (34)$$

and the heat capacity C is then found from Eq. (8). The thermodynamic entropy is obtained by integrating Eq. (9)

$$S_{\text{th}} = \int_0^T \frac{1}{\tau} C d\tau . \quad (35)$$

The BCS equations [1, 23] are recovered from Eqs. (27) and (29) by neglecting the QNF $\delta \mathcal{N}_j^2$ [i.e. $\delta \Delta_j = 0$ in Eq. (27)] together with the pair correlators $\langle \mathcal{A}_j^\dagger \mathcal{A}_{j' \neq j}^\dagger \rangle$ and $\langle \mathcal{A}_j^\dagger \mathcal{A}_{j'} \rangle$ in Eq. (31), and assuming n_j to have the form of Fermi-Dirac distribution for noninteracting quasiparticles, i.e. setting

$$n_j = n_j^{\text{FD}} \equiv \frac{1}{e^{\beta E_j} + 1} . \quad (36)$$

The BCS is known to violate the particle number. This causes a certain quantal particle-number fluctuation around the average value determined by Eq. (29) even at $T = 0$. The FT-BCS1+SCQRPA takes into account only the thermal effect in terms of QNF $\delta \mathcal{N}_j^2$, but does not remove the quantal fluctuation, which is a feature inherent in the BCS wave functions. To cure this inconsistency, a proper particle-number projection (PNP) needs to be carried out. The Lipkin-Nogami (LN) method [25] is an approximated PNP before variation, which is widely used in nuclear study because of its simplicity. This method has been implemented into the FTBCS1+SCQRPA, and the ensuing approach is called the FTLN1+SCQRPA (See Sec. II.C.2. of Ref. [9]). However, the LN method can approximately eliminate only the quantal fluctuations due to particle-number violation within the BCS theory. These quantal fluctuations are different from the thermal particle-number fluctuations, which always arise from the exchange of particles between the systems in the GCE. The LN method is, therefore, not sufficient to remove the particle-number fluctuations within the GCE. To avoid the thermal particle-number fluctuations, the average in the CE should be used instead. Unfortunately, the methods of equilibrium statistical physics applied to the nuclear theories such as the Matsubara-Green's function and/or double-time Green's function techniques, which are used to derived the BCS and QRPA equations at finite temperature, are all based on the GCE. The complete particle-number projection based on the applying particle-number projection operator [26] at finite temperature for these approaches still remains a subject under study [See, e.g. Ref. [27]].

In this paper, the numerical results obtained within both particle-number unprojected (FTBCS1+SCQRPA) and projected (FTLN1+SCQRPA) approaches will be compared with those given by averaging the exact pairing solution with the principal thermodynamic ensembles.

IV. NUMERICAL RESULTS

A. Details of numerical calculations

The schematic model employed for numerical calculations consists of N particles, which are distributed over $\Omega = N$ doubly-folded equidistant levels (i.e. with the level degeneracy $2\Omega_j = 2$). These levels, whose energies are $\epsilon_j = \epsilon[j - (\Omega + 1)/2]$ ($j = 1, \dots, \Omega$), interact via the pairing force with a constant parameter G . The model is half-filled, namely, in the absence of the pairing interaction, all the lowest $\Omega/2$ levels (with negative single-particle energies) are filled up with N particles, leaving $\Omega/2$ upper levels (with positive single-particle energies) empty³. It is worth mentioning that the extension of the exact solution to $T \neq 0$ is not possible at a large value of $\Omega = N$. For the present schematic model, the number of eigenstates n_S , each of which is 2^S -degenerated, increases almost exponentially with Ω

$$n_S(\Omega) = C_{N_{\text{pair}}}^{\Omega} + \sum_S C_S^{\Omega} \times C_{N_{\text{pair}} - \frac{S}{2}}^{\Omega - S}, \quad (37)$$

where $C_n^m = m!/[n!(m - n)!]$ and $N_{\text{pair}} = N/2$ is the numbers of pairs distributed over Ω single-particle levels. The sum in Eq. (37) runs over all the values of total seniorities $S = 0, 2, \dots, \Omega$. Therefore, at $\Omega = N = 16$ there are 5196627 states, which corresponds to the order $\sim 2.7 \times 10^{13}$ for the square matrix to be diagonalized. This makes the finite-temperature extension of the exact pairing solution practically impossible for $\Omega > 16$ since all the eigenvalues must be included in the partition function. Therefore, in the present paper, we limit the calculations up to $\Omega = N = 14$, for which there are 73789 eigenstates. For the GCE average with respect to the system with N particles and $\Omega = N$ levels, the sum over particle numbers n runs from $n_{\text{min}} = 1$ to $n_{\text{max}} = 2\Omega - 1$ with the blocking effect caused by the odd particle properly taken into account. The calculations are carried out by

³ This model is also called Richardson's model, picket-fence model, ladder model, multilevel pairing model, etc. in the literature.

using the level distance $\epsilon = 1$ MeV and the pairing interaction parameter $G = 0.9$ MeV. With these parameters, the values of the pairing gap obtained at $T = 0$ are equal to around 3, 3.5, and 4.5 MeV for $N = 8, 10$, and 12 in qualitative agreement with the empirical systematic for realistic nuclei [16].

B. Results within GCE, CE and BCS-based approaches

Shown in Fig. 1 are the pairing gaps, total energies, and heat capacity obtained for $N = 8, 10$, and 12 as functions of temperature T within the FTBCS, FTBCS1+SCQRPA, and FTLN1+SCQRPA, along with the corresponding results obtained by embedding the exact solutions (eigenvalues) of the Hamiltonian (1) in the CE and GCE. These latter results using the exact pairing solutions are referred to as CE and GCE results hereafter. For the FTBCS1+SCQRPA and FTLN1+SCQRPA the level-weighted gaps $\overline{\Delta}$ (33) are plotted in Figs. 1 (a1) – 1 (a3).

It is seen from this figure that the GCE results are close to the CE ones for the gaps, obtained from Eq. (18), as well as for the total energies, obtained by using Eq. (8). Among three systems under consideration, the largest discrepancies between the CE and GCE results are seen in the lightest system ($N = 8$), for which the GCE gap is slightly lower than the CE one, and consequently, the GCE total energy is slightly higher than that obtained within the CE. As N increases, the high- T values of the GCE and CE gaps become closer, so do the corresponding total energies. Different from the BCS results (dotted lines), which show a collapse of the gap and a spike in the temperature dependence of the heat capacity at $T = T_c$, no singularity occurs in the GCE and CE results. Both GCE and CE gaps decrease monotonously with increasing T and remain finite even at $T \gg 5$ MeV. The FTBCS1+SCQRPA and FTLN1+SCQRPA predictions for the pairing gap are found in qualitative agreement with the GCE and CE results [Figs. 1 (a1) – 1 (a3)]. Because of a different definition of the pairing gap in the exact solutions within the GCE and/or CE, where actually no mean-field gap exists (See Sec. II C1), one cannot expect a more quantitative agreement between the predictions by the FTLN1+SCQRPA and the GCE (CE) results. In this respect, the modified gap (24) yields a better quantitative agreement with the GCE (CE) results, as will be seen later in Sec. IV D. The two BCS-based approaches differ noticeably only at $T \leq T_c$, where the FTLN1+SCQRPA gap, due to PNP, practically

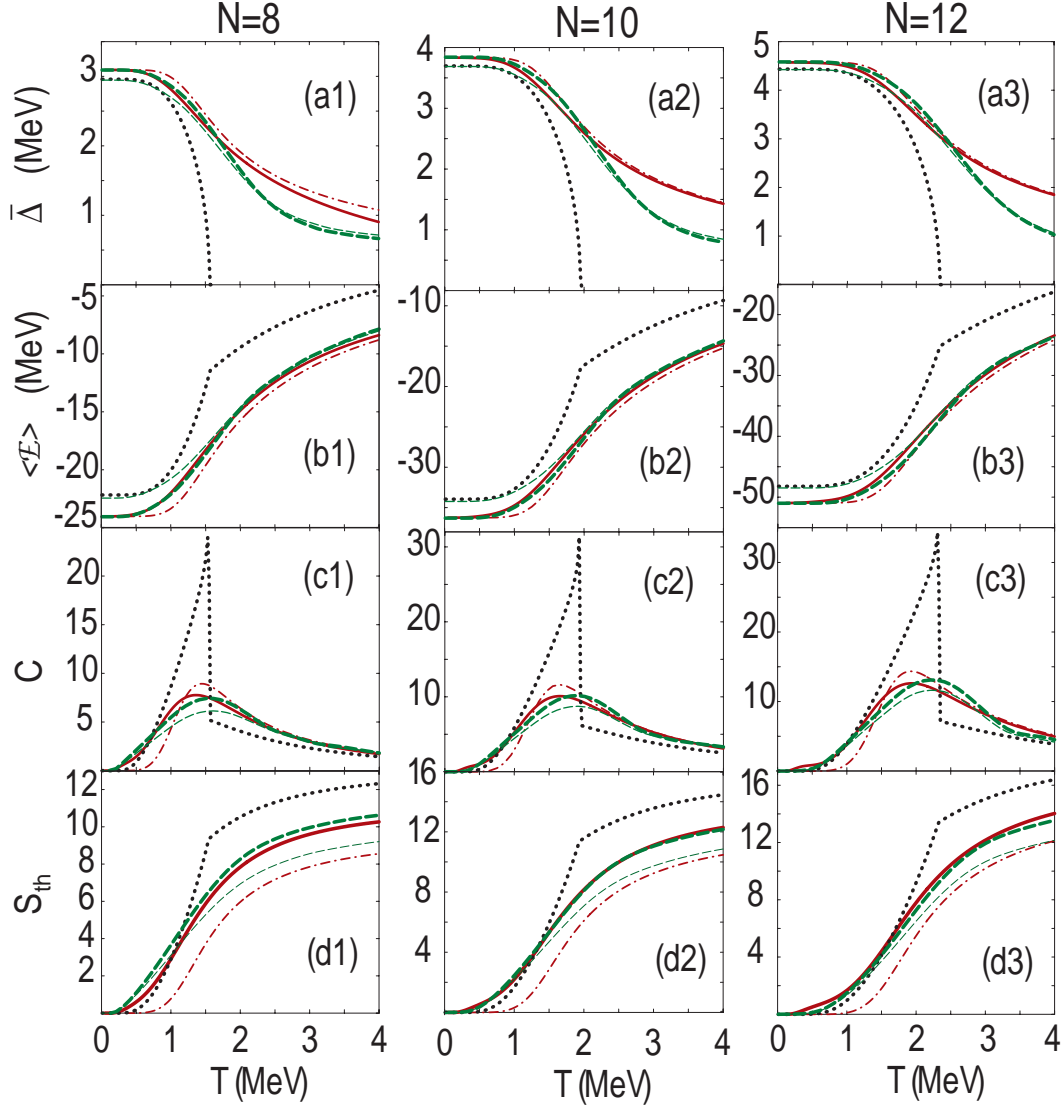


FIG. 1: (Color online) Pairing gaps $\bar{\Delta}$, total energies $\langle \mathcal{E} \rangle$, heat capacities C and thermodynamic entropies, obtained for $N = 8, 10$, and 12 ($G = 0.9$ MeV) within the FTBCS (dotted lines), FTBSC1+SCQRPA (thin dashed lines), FTLN1+SCQRPA (thick dashed lines), CE (dash-dotted lines), and GCE (solid lines) vs temperature T .

coincides with the GCE and CE results at $T < 0.5 - 1$ MeV. At $T > T_c$ the predictions by two approaches start to converge to the same value, which decreases with increasing T , remaining smaller than the GCE and CE gaps.

For the same reason, at $T < T_c$, where the total energy predicted by the FTLN1+SCQRPA agrees very well with the GCE and CE results, the FTBSC1+SCQRPA

energy is significantly larger [Figs 1 (b1) – 1 (b3)]. At $T > T_c$, one finds a remarkable agreement between the energies predicted by the FTBCS1+SCQRPA, FTLN1+SCQRPA, and that obtained within the GCE. This seems to be a natural consequence, given the fact that the two BCS-based approaches are derived by using the variational procedure within the GCE. The energies do not suffer either from the difference in the definitions as the pairing gaps do, as has been discussed above. For the heat capacities [Figs 1 (c1) – 1 (c3)], the spike obtained at $T = T_c$ within the FTBCS theory is completely smeared out within the GCE, CE as well as the FTBCS1+SCQRPA and FTLN1+SCQRPA, where only a broad bump is seen in a large temperature region between 0 and 3 MeV. At $T < 1 - 1.2$ MeV, the difference between the GCE and CE energies leads to a significant discrepancy between the GCE and CE values for the heat capacity. As the FTBCS1+SCQRPA and FTLN1+SCQRPA heat capacities are close to the GCE values, this explains the discrepancy reported in Figs. 4 (b) and 4 (c) of Ref. [9] between these results and the predictions obtained within the CE by the quantum Monte-Carlo calculations, which use a model Hamiltonian with same monopole pairing interaction. The thermodynamic entropies S_{th} are shown as functions of T in Figs. 1 (d1) – 1 (d3). Once again the FTLN1+SCQRPA results for the thermodynamic entropy S_{th} agree very well with S_{th} obtained within the GCE, whereas such good agreement is seen for the FTBCS1-SCQRPA results only at $T < 1$ MeV. The CE thermodynamic entropy is significantly lower than the values obtained in all other approaches under consideration, which are based on averaging within the GCE. On the other hand, the BCS theory strongly overestimates the thermodynamic entropy at $T > T_c$.

C. Results within MCE

The values of temperature within the MCE as extracted by using Eq. (13) are plotted in Fig. 2 along with the CE results against the excitation energy \mathcal{E}^* . The CE definition of the latter is $\mathcal{E}_C^* \equiv \langle \mathcal{E}(T) \rangle_C - \langle \mathcal{E}(T = 0) \rangle_C$. For comparison, the results obtained by using the entropy (17) are also presented in the top panels [Figs. 2 (a) – 2 (c)]. They show the values of the eigenstate temperatures T_s , which scatter widely around the heat bath temperature (i.e. the CE result) [Figs. 2 (a) – 2 (c)]. Many of these values are even negative. Since the eigenstate temperatures T_s are related with the spread of the exact eigenfunctions over the “unperturbed” basis states k with the weights $[C_k^{(s)}]^2$, they need not follow the trend

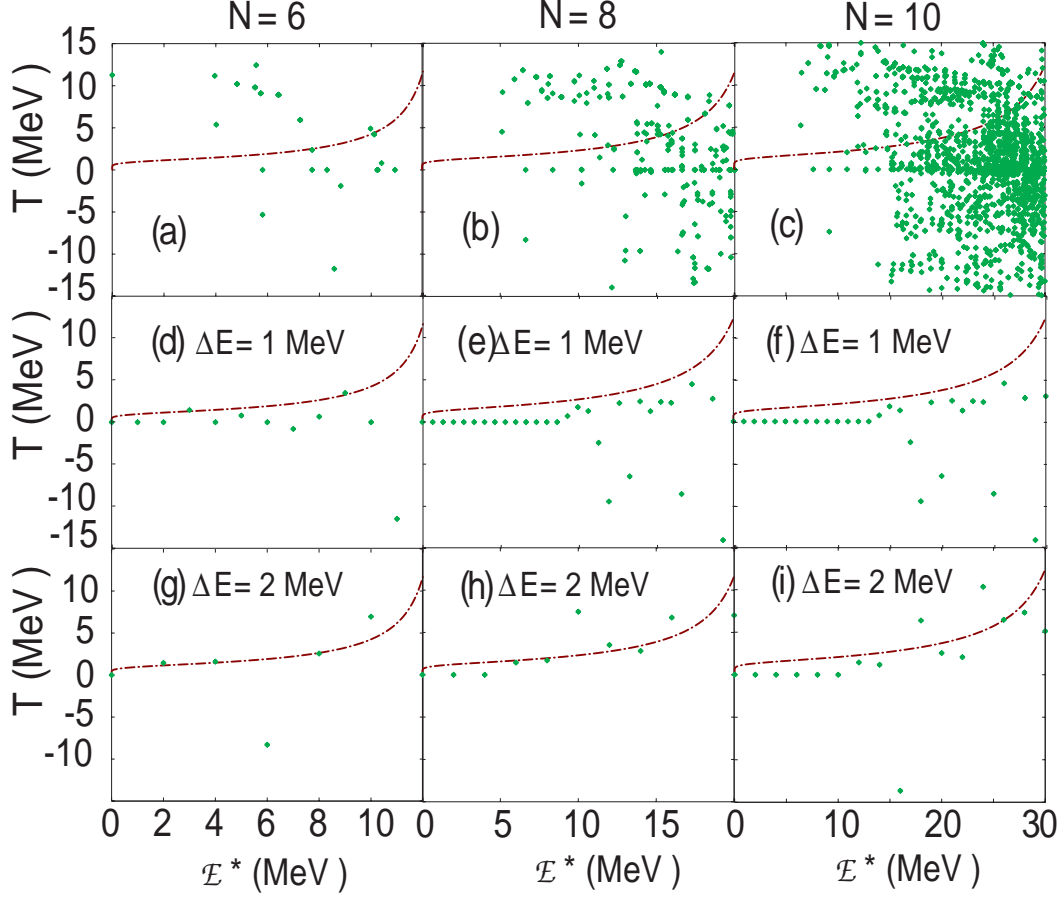


FIG. 2: (Color online) Temperature extracted from Eq. (13) within the MCE (dots) vs excitation energy \mathcal{E}^* in comparison with the CE results (dash-dotted line) for $N = 8, 10$, and 12 . The results in the top panels, (a) – (c), are obtained from the definition of Neumann for entropy Eq. (15), whereas those in the middle panels, (d) – (f), and bottom ones, (g) – (i), are calculated from Boltzmann’s entropy Eq. (12) with two different values of the energy interval ΔE in the statistical weight Ω .

of the heat bath (or canonical) temperature, which depends just on the level density [Eqs. (12) and (13)]. In fact, with increasing the energy interval ΔE , within which the levels are counted, the values of the MCE temperature determined by Eq.(13) gradually converge to the CE values [Figs. 2 (a) – 2 (i)]. This means that, the thermal equilibrium within the MCE for the present isolated pairing model can be reached only at large N and dense spectrum (small level spacing). Moreover, a full thermalization in a system with pure pairing is a subject under question. In Ref. [7, 28], the thermalization of the system is characterized

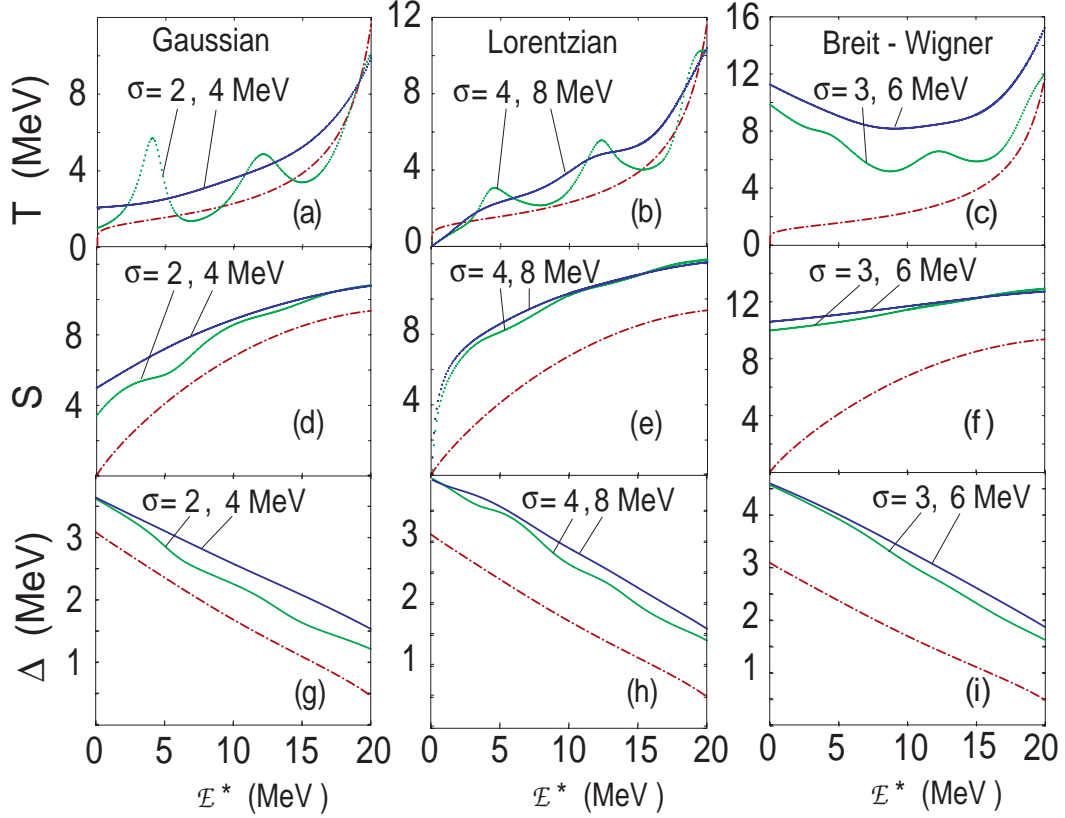


FIG. 3: (Color online) Temperatures [(a) – (c)], entropies [(d) – (f)], and pairing gaps [(g) – (i)] within the MCE as functions of excitation energy \mathcal{E}^* for $N = 8$ ($G = 0.9$ MeV) obtained by using the Gaussian, Lorentz, and Breit-Wigner distributions from Eq. (14) for the level density at different values of the parameter σ . The dash-dotted lines show the CE values.

by the single-particle temperature, which is obtained by fitting the occupation numbers of the individual eigenstates to those given by the Fermi-Dirac distribution. The numerical results Fig. 12 of Ref. [28] show that, the temperature extracted from the density of states in ^{116}Sn by using Eq. (13) agrees with the single-particle temperature only when all the residual interactions are taken into account. With the pure pairing interaction alone, the single-particle temperature shows a low temperature of the whole system, whereas the MCE temperature (13) is a hyperbola as a function of the excitation energy with a singularity in the middle of the spectrum, where it turns negative [See also Figs. 53 and 54 of Ref. [7]].

The values of MCE temperature, entropy and gap obtained by using the Gaussian, Lorentz, and Breit-Wigner distributions from Eq. (14) are shown in Fig. 3 as functions of excitation energy \mathcal{E}^* . While the fluctuating behavior of the microcanonical temperature

can be smoothed out by increasing the parameter σ in all three distributions, we found that only the Gaussian distribution can simultaneously fit both the temperature and entropy [Figs. 3 (a) and 3 (d)]. The Lorentz distribution can fit only the MCE temperature to the CE one, but fails to do so for the entropy [Figs. 3 (b) and 3 (e)], whereas the Breit-Wigner distribution can fit the MCE temperature to the CE value only at high excitation energies [Figs. 3 (c)]. A similar result is seen for the pairing gaps as functions of \mathcal{E}^* , where the Gaussian fit gives the best performance among the three distributions [Compare Figs. 3 (g), 3 (h), and 3 (i)]⁴. We conclude that the Gaussian distribution should be chosen as the best one for smoothing the level density $\rho(\mathcal{E})$ in Eq. (5) to extract the MCE temperature.

D. Pairing gaps extracted from odd-even mass differences

We extracted the pairing gaps $\Delta^{(i)}(\beta, N)$ ($i = 3$ and 4) by using the simple extension of the odd-even mass formula to $T \neq 0$ in Eq. (19) as well as the modified gaps $\tilde{\Delta}^{(i)}(\beta, N)$ from Eq. (24), and the canonical gaps $\Delta_C^{(i)}$ from Eq. (18) for several particle numbers up to $N = 12$. In these calculations, the blocking effect caused by the unpaired particle in the systems with an odd particle number is properly taken into account in constructing the basis states when diagonalizing the pairing Hamiltonian. The results obtained for $N = 9$ and 10 ($\Omega = 10$) are displayed in Fig. 4. First of all, the values for S' are found to be always negative, and increases with $T > 1$ MeV to reach a value of around -2 MeV at $T = 5$ MeV, and vanish at very high T . By comparing Figs. 4 (a) and 4 (b) one can see a clear manifestation of the parity effect [18], which causes the reduction of the three-point gap the in the system with an odd particle number ($N = 9$) due to the blocking effect. For lights systems as those considered here, this reduction is rather strong (about 1 MeV at $T = 0$). With increasing T , as the thermodynamics weakens the effect of a single-unpaired particle, the parity effect starts to fade out in such a way that the three-point canonical gap $\Delta_C^{(3)}(N = 9)$ slightly increases with T up to $T \simeq 1$ MeV, starting from which it is even slightly larger than $\Delta_C^{(4)}(N = 9)$. This feature is found in qualitative agreement with the

⁴ The non-vanishing values of T and S at $\mathcal{E}^* = 0$ in Figs. 3 (a), 3 (c), 3 (d), 3 (f) are the artifacts due to the use of the Gaussian and Breit-Wigner distribution functions (14) to smooth out the discrete level density. These two distributions have non-zero values $\sim 1/\sigma$ at $x = 0$, where the Lorentz distribution vanishes.

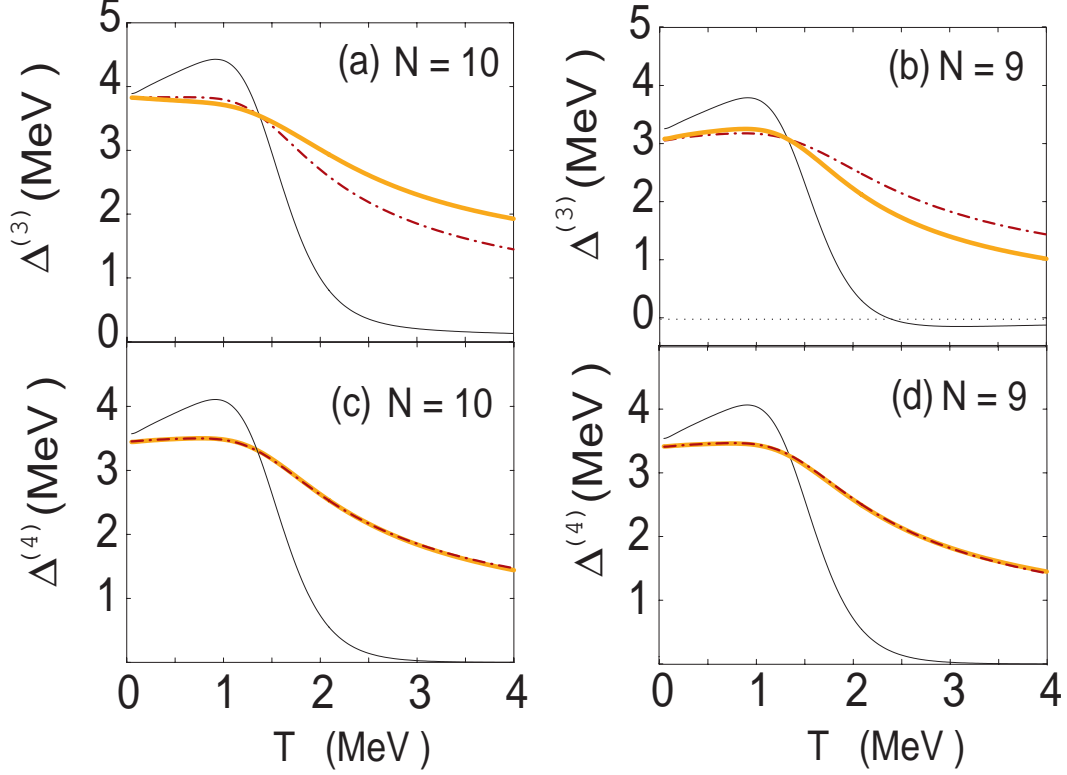


FIG. 4: (Color online) Pairing gaps extracted from the odd-even mass differences as functions of T for $N = 10$ (a,c) and $N = 9$ (b,d) ($\Omega = 10$, $G = 0.9$ MeV). The thin solid and thick solid lines denote the gaps $\Delta^{(i)}(\beta, N)$ ($i = 3, 4$) from Eq. (19), and the modified gaps $\tilde{\Delta}^{(i)}(\beta, N)$ from Eq. (24), respectively. The dash-dotted lines are the canonical results $\Delta_C^{(i)}$. The upper panels (a) and (b) show the three-points gaps ($i = 3$), whereas the corresponding four-points gaps ($i = 4$) are shown in the lower panels (c) and (d).

results obtained in Fig. 25 of Ref. [18] for ultrasmall metallic grains. It is also seen in Fig. 4 that the naive extension of the odd-even mass formula to $T \neq 0$, resulting in the gap $\Delta^{(i)}(\beta, N)$ (thin solid lines), fails to match the temperature-dependence of the canonical gap $\Delta_C^{(i)}$ (dash-dotted lines). The former even increases with T at $T < 1$ MeV, whereas it drastically drops at $T > 1 - 1.5$ MeV, resulting in a very depleted tail at $T > 2$ MeV as compared to the canonical gap $\Delta_C^{(i)}$. Moreover, the three-point gap $\Delta^{(3)}(\beta, N = 9)$ even turns negative at $T > 2.4$ MeV, suggesting that such simple extension of the odd-even mass difference to finite T is invalid. At the same time, the modified gap $\tilde{\Delta}^{(i)}(\beta, N)$ (thick solid line) given by Eq. (24) is found in much better agreement with the canonical one. At $T < 1.5$ MeV, the three point-gap $\tilde{\Delta}^{(3)}(\beta, N)$ is almost the same as the canonical gap. At higher

T , it becomes larger (smaller) than the canonical value for the system with an even (odd) N , however the systematic of the results of our calculations up to $N = 12$ show we that this discrepancy decreases with increasing the particle number. The source of the discrepancy resides in the assumption of the odd-even mass formula that the gap obtained as the energy difference between the systems with $N + 1$ and N particles is the same as that obtained from the energy difference between systems with N and $N - 1$ particles. This assumption does not hold for small N (Cf. Ref. [29]). The average in the four-point gap nearly eliminates this difference. As a result, the modified four-point gaps $\tilde{\Delta}^{(4)}(\beta, N)$ practically coincide with the canonical gaps. A natural consequence of the average in the definition of the four-point gap (20) is that the gaps obtained in the systems with N and $N - 1$ particles are now nearly the same. The pairing gaps predicted by a number of alternative theories [3, 4, 5, 6, 8], including those discussed in the present work, are in closer agreement to the GCE and CE gaps rather than to the gap $\Delta(\beta, N)$ from Eq. (19). Therefore, the comparison in Fig. 4 suggests that formula (24) is a much better candidate for the experimental gap at $T \neq 0$, rather than the simple odd-even mass difference (19).

V. CONCLUSIONS

In the present work, a systematic comparison is conducted for pairing properties of finite systems at finite temperature as predicted by the exact solutions of the pairing problem embedded in three principal statistical ensembles, as well as by the recently developed FTBCS1 (FTLN1)+SCQRPA. The analysis of numerical results obtained within the doubly-folded equidistant multilevel model for the pairing gap, total energy, heat capacity, entropies, and MCE temperature allows us to draw following conclusions.

1) The sharp SN phase transition is indeed smoothed out in exact calculations within all three principal ensembles. The results obtained within GCE and CE are very close to each other even for systems with small number of particles. As for the MCE, although it can also be used to study the pairing properties of isolated systems at high-excitation energies, there is a certain ambiguity in the temperature extracted from the level density due to the discreteness of a small-size system. This ambiguity, therefore, depends on the shape and parameter of the distribution employed to smooth the discrete level density. We found that, in this respect, the normal (Gaussian) distribution gives the best fit for both of the temperature

and entropy to the canonical values. The wide fluctuations of MCE temperature obtained here also indicate that thermal equilibrium within thermally isolated pure-pairing systems might not be reached. On the other hand, it opens an interesting perspective of studying the behavior of phase transitions in finite systems within microcanonical thermodynamics [30] by using the exact solutions of pairing problem.

2) The predictions by the FTBCS1+SCQRPA and FTLN1+SCQRPA are found in reasonable agreement with the results obtained by using the exact solutions embedded in the GCE and CE. The best agreement is seen between the FTLN1+SCQRPA and the GCE results. Once again, this is a robust confirmation that quasiparticle-number fluctuation, included in these approximations, is indeed the microscopic origin of the strong thermal fluctuations that smooth out the sharp SN phase transition in finite systems.

3) We suggest a novel formula to extract the pairing gap at finite temperature from the difference of total energies of even and odd systems where the contribution of uncorrelated single-particle motion is subtracted. The new formula predicts a pairing gap in much better agreement with the canonical gap than the simple finite-temperature extension of the odd-even mass formula.

Acknowledgments

Discussions with Peter Schuck (Orsay) are gratefully acknowledged. One of us (N.Q.H.) also thanks S. Frauendorf (Notre Dame), and V. Zelevinsky (East Lansing) for discussions and hospitality during his visit at the University of Notre Dame and Cyclotron Institute of the Michigan State University, where a part of this work was presented.

NQH is a RIKEN Asian Program Associate. The numerical calculations were carried out using the FORTRAN IMSL Library by Visual Numerics on the RIKEN Super Combined Cluster (RSCC) system.

-
- [1] J. Bardeen, L. Cooper, and Schrieffer, Phys. Rev. **108**, 1175 (1957).
 - [2] N.N. Bogoliubov and S.V. Tyablikov, Sov. Phys. Dokl. **4**, 589 (1959) [Dokl. Akad. Nauk. SSSR **126**, 53 (1959)]; D.N. Zubarev, Sov. Phys. Usp. **3**, 320 (1960) [Usp. Fiz. Nauk **71**, 71 (1960);

- R. Kubo, M. Toda, and N. Hashitsume, *Statistical Physics II - Nonequilibrium Statistical Mechanics* (Springer, Berlin-Heidelberg, 1985).
- [3] L.G. Moretto, Phys. Lett. B **40**, 1 (1972).
 - [4] A.L. Goodman, Phys. Rev. C **29**, 1887 (1984).
 - [5] J.L. Egido, P. Ring, S. Iwasaki, and H.J. Mang, Phys. Lett. B **154**, 1 (1985).
 - [6] R. Rossignoli, P. Ring and N.D. Dang, Phys. Lett. B **297**, 9 (1992); N.D. Dang, P. Ring and R. Rossignoli, Phys. Rev. C **47**, 606 (1993).
 - [7] V. Zelevinsky, B.A. Brown, N. Frazier, and M. Horoi, Phys. Rep. **276**, 85 (1996).
 - [8] N. Dinh Dang and V. Zelevinsky, Phys. Rev. C **64**, 064319 (2001); N.D. Dang and A. Arima, Phys. Rev. C **67**, 014304 (2003); N.D. Dang and A. Arima, Phys. Rev. C **68**, 014318 (2003); N.D. Dang, Nucl. Phys. A **784**, 147 (2007).
 - [9] N.D. Dang and N.Q. Hung, Phys. Rev. C **77**, 064315 (2008).
 - [10] N.Q. Hung and N.D. Dang, Phys. Rev. C **78**, 064315 (2008).
 - [11] R.W. Richardson, Phys. Lett. **3**, 277 (1963); Ibid. **14**, 325 (1965); R.W. Richardson and N. Sherman, Nucl. Phys. **52**, 221 (1964).
 - [12] A. Volya, B.A. Brown, and V. Zelevinsky, Phys. Lett. B 509 (2001) 37.
 - [13] R. Kubo, J. Phys. Soc. Japan **17**, 975 (1962).
 - [14] R. Denton, B. Mühlischlegel, and D.J. Scalapino, Phys. Rev. B **8**, 3589 (1973).
 - [15] T. Sumaryada and A. Volya, Phys. Rev. C **76**, 024319 (2007).
 - [16] A. Bohr and B.R. Mottelson, *Nuclear structure I* (Bejamin, NY, 1969).
 - [17] P. Ring and P. Schuck, *The Nuclear Many-Body Problem* (Springer, Heidelberg, 2004).
 - [18] J. von Delft and D.C. Ralph, Phys. Rep. **345**, 61 (2001).
 - [19] R. Rossignoli, N. Canozza, and P. Ring, Ann. Phys. **275**, 1 (1999).
 - [20] S. Frauendorf, N.K. Kuzmenko, V.M. Mikhajlov, and J.A. Sheikh, Phys. Rev. B **68**, 024518 (2003).
 - [21] G. Breit, Phys. Rev. **58**, 506 (1940); E.P. Wigner, Phys. Rev. **70**, 15 (1946); M. Danos and W. Greiner, Phys. Rev. **134**, B284 (1964).
 - [22] K. Kaneko and M. Hasegawa, Phys. Rev. C **72**, 024307 (2005), K. Kaneko *et al.*, Phys. Rev. C **74**, 024325 (2006).
 - [23] N.N. Bogoliubov, JETP **34**, 58 (1958).
 - [24] N.Q. Hung and N.D. Dang, Phys. Rev. C **76**, 054302 (2007); **77**, 029905(E) (2008).

- [25] H.J. Lipkin, Ann. Phys. **9**, 272 (1960); Y. Nogami, Phys. Rev. **134**, B313 (1964); H.C. Pradhan, Y. Nogami, and J. Law, Nucl. Phys. A **201**, 357 (1973).
- [26] H. Olofsson, R. Bengtsson, P. Möller, Nucl. Phys. A **784**, 104 (2007).
- [27] N. Dinh Dang, Phys. Rev. C **76**, 064320 (2007).
- [28] A. Volya, V. Zelevinsky, and B. Alex Brown, Phys. Rev. C **65**, 054312 (2002).
- [29] N. Dinh Dang, Phys. Rev. C **74**, 024318 (2006).
- [30] D.H.E. Gross and J.F. Kenney, J. Chem. Phys. **112**, 224111 (2005).